Archives of Mechanics • Archiwum Mechaniki Stosowanej • 31, 2, pp. 875–896, Warszawa 1979

Response of constrained visco-elastic beams to random excitation

O. N. KAUL (SRINAGAR), K. N. GUPTA and B. C. NAKRA (NEW DELHI)

THE PAPER deals with analytical formulations for flexural vibrations of simply supported three-layer beams which have a constrained viscoelastic core and are subjected to random excitation of white noise and turbulent boundary layer types, respectively. By applying the usual analytical techniques of random vibration, the expressions for the mean square displacement response of the beam are obtained in terms of its transfer function and the spectral density of the input process. In the case of turbulent boundary layer excitation, Bull's model is used for the spectral density. The influence of some geometrical and physical parameters on the response has been studied. The response of the sandwich beam has been compared with that of a reference homogeneous beam so as to determine conditions under which minimum response can be obtained. Experiments have been conducted on a few samples of the sandwich beam for both types of excitation and the test results are being compared with the corresponding theoretical results. A reasonable agreement between these results has been observed.

Niniejsza praca dotyczy sformułowań analitycznych dla drgań giętnych swobodnie podpartych trójwarstwowych belek, które mają zamocowany lepkosprężysty rdzeń i poddane są stochastycznemu pobudzaniu typu białego szumu i turbulencyjnej warstwy brzegowej. Stosując zwykłe techniki analityczne drgań stochastycznych otrzymano wyrażenia na średni pierwiastek kwadratowy przesunięcia — odpowiedź belki, w funkcji przepustowości i gęstości spektralnej procesu wejściowego. W przypadku wzbudzenia typu turbulencyjnej warstwy brzegowej dla gęstości spektralnej wykorzystano model Bulla. Zbadano wpływ niektórych parametrów geometrycznych i fizycznych na reakcję. Reakcja warstwowej belki porównana została z reakcją wzorcowej jednorodnej belki dla określenia warunków, przy których otrzymuje się reakcję minimalną. Przeprowadzono eksperymenty na kilku warstwowych belkach dla obu typów wzbudzenia, a wyniki porównano z odpowiednimi wynikami teoretycznymi. Zaobserwowano dobrą zgodność między tymi wynikami.

Настоящая работа касается аналитических формулировок для колебаний изгиба свободно подпертых трехслойных балок, которые имеют закрепленный вязко-упругий стержень и подвергнуты стохастическому возбуждению типа белого шума и турбулентному пограничному слою соответственно. Применяя обычные аналитические техники стохастических колебаний, получены выражения для среднего квадратного корня перемещения — отклик балки, в функции пропускной способности и спектральной плотности входного процесса. В случае возбуждения типа турбулентного пограничного слоя для спектральной плотности использована модель Булла. Исследовано влияние некоторых геометрических и физических параметров на отклик. Отклик слоевой балки сравнен с откликом эталонной однородной балки для определения условий, при которых получается минимальный отклик. Проведены эксперименты на нескольких слоевых балках и результаты сравнены с соответствующими теоретическими результатами. Наблюдалось значительное совпадение между этими результатами.

Notations

a_i area of cross section of i-th layer,
b width of beam,
D operator $\partial/\partial t$,
D_1 operator $\partial/\partial x$,
E_i Young's modulus of i-th layer,

$E[\,]$ mathematical expectation of the random quantity inside the brackets,
$f(x, t)$ external loading of distributed type,
G_2 shear modulus of 2nd layer,
$h_w(n, t)$ impulse response function,
$H_w(n, \omega)$ transfer function,
H_i semi-thickness of i-th layer,
K_i longitudinal stiffness of i-th layer $(=E_i a_i)$,
L length of beam,
M bending moment,
n, m modal number,
$R_w(\tau), R_f(\tau)$ auto-correlation of w and f,
$R_f(\bar{\zeta}, \tau)$ correlation of f for turbulent boundary layer excitation,
S_0 spectral density of white-noise random excitation,
$S_f(\bar{\zeta}, \omega), S_f(\omega)$ spectral density of f,
t time variable,
U_C convection velocity of air,
$\alpha, \beta, \gamma, \psi$ constants of the visco-elastic model,
$\zeta_1, \zeta_2, \eta_2, \eta_3$ elements of the visco-elastic model,
ϱ_i mass density of i-th layer,
μ mass per unit length of beam,
ϕ slope of beam,
ω angular frequency,
τ time delay,
$T_{i,j}$ H_i/H_j,

A dash over a variable represents its derivation with respect to x.

1. Introduction

IN MOST of the modern machines the use of high speed and high power has given rise to a severe vibration environment spread over a wide range of frequencies. This is further augmented by the use of light weight structural members. Such severe vibrations, if not suitably controlled, may result in fatigue failure and malfunctioning of the machine elements and cause noise radiation and discomfort.

Viscoelastic damping materials like long chain polymers, rubbers and plastics, which possess high energy dissipation capacity, have been found most successful in the control of vibrations [1]. These materials are used in a composite construction with a structural member for adding damping to the system either as an unconstrained arrangement or as a constrained arrangement. In the unconstrained arrangement viscoelastic damping layers are applied to the surfaces of the structural member, whereas in the constrained arrangement the viscoelastic material layers are sandwiched between two layers of the structural member. The unconstrained arrangement is particularly useful for adding damping to an existing structural member, while the constrained arrangement has proven to be more suitable for producing integrally damped structural members. Constrained viscoelastic layers provide more damping than unconstrained layers for the same total weight of the structure [2].

Multilayer structures have diverse uses as, for example, in aircraft fuselage structures missile frames, shock attenuation equipment etc. Most of these structures are subjected

to random loads in addition to conditions of free and forced vibrations and shock excitation. Considerable work has been reported on the free and forced vibrations and shock excitation of multilayer structures [2–8], but the work reported on the response of such structures to random excitation has been rather meagre. However, there have been some reports on the response of homogeneous structures to random excitation. The use of viscoelastic damping compound in the control of jet-efflux excited vibrations has been reported by MEAD [9]. This author used a complex modulus representation for representing the dynamic properties of the viscoelastic material: however this is applicable to harmonic excitation only. SAUNDERS [10] has determined the response of multilayer plates to spatially-distributed random force. The light damping assumption made by him in his analysis is not applicable to constrained viscoelastic layers.

In this paper the response of constrained viscoelastic beams (3-layer types) to random excitation is determined. Two types of random excitation, namely the "white-noise" type and the „turbulent boundary layer" type, are considered. The effect of various geometrical and physical parameters on the response is evaluated and simply supported end conditions are considered. Some experimental results are also reported.

2. Equation of motion of a general three-layer sandwich beam

The equation of motion for a three-layer beam, shown in Fig. 1, has been derived in [11, 12] on lines similar to those of DI TARANTO [4]. These are based on the following assumptions:

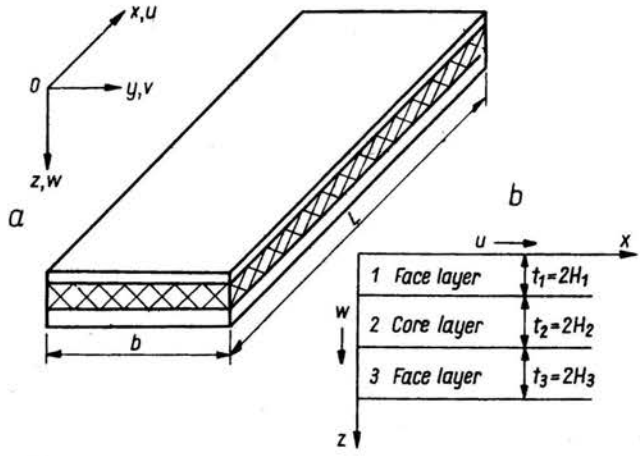

FIG. 1. Three-layer laminated beam. a) Layer arrangement.

i) The face layers bend according to the Bernoulli-Euler theory.

ii) No slipping occurs at the interfaces of the layer when the beam bends.

iii) In face layers only extensional and bending effects occur while shear deformations are negligible.

iv) Transverse displacement at a transverse section is constant along the thickness.

v) Longitudinal displacement at a transverse section varies linearly with layer thickness but its rate is different in different layers.

vi) All displacements are small and conform to the linear theory of elasticity.

vii) Rotational and longitudinal inertia terms are negligible and only transverse inertia terms are included.

viii) The material of the viscoelastic layer is linear, i.e. its characteristics are strain independent and its dynamic properties are represented by a 4-element model.

These equations of motion are derived by first considering the equilibrium of forces (Fig. 2) and the assumed pattern of deformation (Fig. 3). From these we have

$$D_1^2 M = \mu D^2 w - f(x,t), \tag{2.1}$$

$$\phi = \frac{u_1 s}{\delta_1} - \frac{u_1''}{r_1 \delta_1}, \tag{2.2}$$

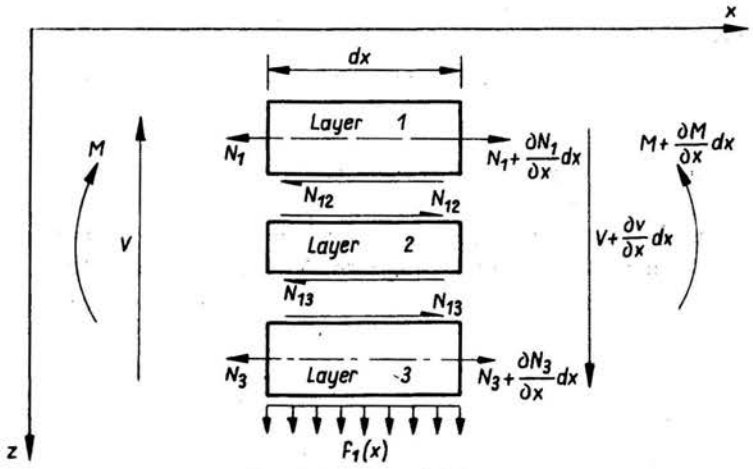

FIG. 2. Force qeuilibrium.

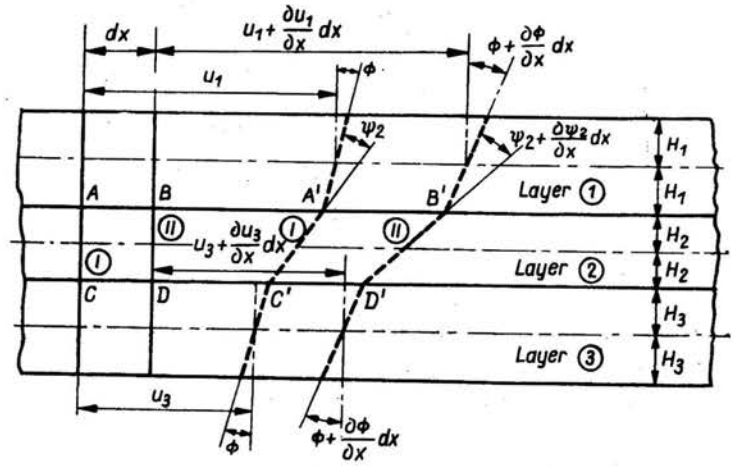

FIG. 3. Relative deformations in the composite beam.

and

$$M = -(K_1 \delta_1 u_1' + K\phi'), \tag{2.3}$$

where

$$\begin{aligned} s &= (K_1+K_3)/K_3, \\ \delta_1 &= H_1+2H_2+H_3, \\ r_1 &= G_2 b/(2H_2 K_1), \\ K &= K_1+K_3. \end{aligned} \tag{2.4}$$

Substituting the value of M from Eq. (2.3) into Eq. (2.1), we obtain

$$K_1 \delta_1 u_1''' + K\phi''' + \mu D^2 w = f(x, t). \tag{2.5}$$

Differentiating both sides of Eq. (2.2) three times with respect to x and rearranging, we get

$$u_1''' = r_1 \delta_1 (r_1 s - D_1^2)^{-1} \phi'''. \tag{2.6}$$

Substituting from Eq. (2.6) into Eq. (2.5), we get after simplification the following equation:

$$\{r_1 K_1 \delta_1^2 + (r_1 s - D_1^2) K\}\phi''' + \mu(r_1 s - D_1^2) D^2 w = (r_1 s - D_1^2) f(x, t). \tag{2.7}$$

But

$$\phi = \frac{\partial w}{\partial x} = D_1 w,$$

therefore

$$\phi''' = D_1^4 w. \tag{2.8}$$

Using Eq. (2.8) in Eq. (2.7) and dividing both sides by K and putting $\bar{x} = x/L$, we get the following equation of motion in the non-dimensional form for a general three-layer sandwich beam, when undergoing flexural vibrations:

$$\frac{\partial^6 w}{\partial \bar{x}^6} - J_1(1+Y)\frac{\partial^4 w}{\partial \bar{x}^4} + P\frac{\partial^4 w}{\partial \bar{x}^2 \partial t^2} - PJ_1 \frac{\partial^2 w}{\partial t^2} = P_1 \frac{\partial^2 f(\bar{x}, t)}{\partial \bar{x}^2} - P_1 J_1 f(\bar{x}, t), \tag{2.9}$$

where

$$\begin{aligned} J_1 &= r_1 s = \frac{bL^2 s}{2H_2 H_1} G_2 = CG_2, \\ Y &= K_1 \delta_1^2/(sK), \\ P_1 &= L^4/K, \\ P &= P_1 \mu, \\ C &= bL^2 s/(2H_2 K_1). \end{aligned} \tag{2.10}$$

3. Sandwich beam having a viscoelastic core

3.1. Equation of motion

The core layer is assumed to be of a linear viscoelastic material with its dynamic properties in shear represented by a four-element model of the type shown in Fig. 4.

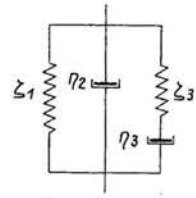

FIG. 4. Four-element viscoelastic model.

The dynamic shear modulus G_2 of the viscoelastic material is [12]

$$G_2 = \frac{\beta+\gamma D+\psi D^2}{1+\alpha D}, \tag{3.1}$$

where α, β, γ and ψ are the model constants and their values in terms of the elements of the model are

$$\begin{aligned} &\alpha = \eta_3/\zeta_3, \quad \beta = \zeta_1, \\ &\gamma = \eta_2+\eta_3+\zeta_1\eta_3/\zeta_3, \quad \psi = \eta_2\eta_3/\zeta_3. \end{aligned} \tag{3.2}$$

Substituting the value of G_2 from Eq. (3.1) into Eq. (2.9) and rearranging, the following equation of motion of a three-layer sandwich beam having a viscoelastic core is obtained:

$$\begin{aligned} (1+\alpha D)\frac{\partial^6 w}{\partial \bar{x}^6} - C(1+Y)(\beta+\gamma D+\psi D^2)\frac{\partial^4 w}{\partial \bar{x}^4} + P(1+\alpha D)\frac{\partial^4 w}{\partial \bar{x}^2 \partial t^2} \\ - PC(\beta+\gamma D+\psi D^2)\frac{\partial^2 w}{\partial t^2} = P_1(1+\alpha D)\frac{\partial^2 f(\bar{x}, t)}{\partial \bar{x}^2} - P_1 C(\beta+\gamma D+\psi D^2) f(\bar{x}, t). \end{aligned} \tag{3.3}$$

3.2. Transfer function

The transfer function of the system (i.e. the beam) is obtained from its equation of motion assuming the external loading $f(\bar{x}, t)$ to be of the form

$$f(\bar{x}, t) = e^{i\omega t}\sin n\pi\bar{x} \tag{3.4}$$

and the displacement response $w(\bar{x}, t)$ of the form

$$w(\bar{x}, t) = H_w(n, \omega)\, e^{i\omega t}\sin n\pi\bar{x} \tag{3.5}$$

which satisfies the end conditions of a simply supported beam. $H_w(n, \omega)$ is termed as the transfer function of the beam. Substituting Eqs. (3.4) and (3.5) into Eq. (3.3), the following is obtained:

$$H_w(n, \omega) = \frac{-\omega^2 B_2 + i\omega B_1 + B_0}{\omega^4 A_4 - i\omega^3 A_3 - \omega^2 A_2 + i\omega A_1 + A_0}, \tag{3.6}$$

where

$$\begin{aligned} &B_2 = C\psi P_1, \quad B_1 = (\alpha n^2\pi^2 + C\gamma)P_1, \\ &B_0 = (n^2\pi^2 + C\beta)P_1, \quad A_4 = \mu B_2, \\ &A_3 = \mu B_1, \quad A_2 = \mu B_0 + n^4\pi^4 C\psi(1+Y), \\ &A_1 = n^6\pi^6\alpha + n^4\pi^4 C\gamma(1+Y), \quad A_0 = n^6\pi^6 + n^4\pi^4 C\beta(1+Y). \end{aligned} \tag{3.7}$$

3.3. Determination of response

To obtain the response to a random loading the impulse response function $h_w(n, t)$ is first determined from the system transfer function $H_w(n, \omega)$ by the relation

$$h_w(n, t) = \frac{1}{2\pi} \int_{-\infty}^{\infty} H_w(n, \omega) e^{i\omega t} d\omega. \tag{3.8}$$

The displacement response $w(\bar{x}, t)$ corresponding to the excitation $f(\bar{x}, t)$ is now obtained in terms of the impulse response function by using the convolution integral [13] as

$$w(\bar{x}, t) = \int_{-\infty}^{\infty} f(\bar{x}, \tau) h_w(n, t-\tau) d\tau. \tag{3.9}$$

Since the transfer function Eq. (3.6) is based on a loading whose space variation is $\sin n\pi\bar{x}$, we decompose the loading also into similar space modes and so we write

$$f(\bar{x}, t) = \sum_{n=1}^{\infty} f_n(t) \sin n\pi\bar{x}, \tag{3.10}$$

where

$$f_n(t) = 2 \int_0^1 f(\bar{x}, t) \sin n\pi\bar{x} d\bar{x}. \tag{3.11}$$

Combining Eqs. (3.9), (3.10) and (3.11), we get

$$w(\bar{x}, t) = \sum_{n=1}^{\infty} \sin n\pi\bar{x} \int_{-\infty}^{\infty} h_w(n, t-\tau)\, 2 \int_0^1 f(\bar{\xi}, \tau) \sin n\pi\bar{\xi} d\bar{\xi} d\tau. \tag{3.12}$$

Equation (3.12) represents the formal solution for the response to each sample excitation.

The statistical average over the sample space of the product $w(\bar{x}_1, t_1) \cdot w(\bar{x}_2, t_2)$ which reduces to the mean square of w, when $\bar{x}_2 = \bar{x}_1$, $t_2 = t_1$, is given by

$$E[w(\bar{x}_1, t_1) \cdot w(\bar{x}_2, t_2)] = \sum_{n=1}^{\infty} \sum_{m=1}^{\infty} \sin n\pi\bar{x}_1 \sin m\pi\bar{x}_2 \times \int_{-\infty}^{\infty} \int_{-\infty}^{\infty} h_w(n, t_1-\tau_1) \cdot h_w(m, t_2-\tau_2) \cdot 4 \int_0^1 \int_0^1 E[f(\bar{\xi}_1, \tau_1) \cdot f(\bar{\xi}_2, \tau_2)] \times \sin n\pi\bar{\xi}_1 \sin m\pi\bar{\xi}_2 d\bar{\xi}_1 d\bar{\xi}_2 d\tau_1 d\tau_2. \tag{3.13}$$

Equation (3.13) shows that the statistical average of the response is related to a similar statistical average of the excitation.

3.3.1. White-noise random excitation

(i) *Distributed load type*

Let the excitation process be stationary and be such that spacewise it is completely uncorrelated, but timewise there exists some correlation, i.e. the term $E[f(\bar{\xi}_1, \tau_1) \cdot f(\bar{\xi}_2, \tau_2)]$ can be expressed as

$$E[f(\bar{\xi}_1, \tau_1) \cdot f(\bar{\xi}_2, \tau_2)] = R(\tau_1 - \tau_2)\, \delta(\bar{\xi}_1 - \bar{\xi}_2), \tag{3.14}$$

where δ is the Dirac's delta function. Now, substituting Eq. (3.14) and putting $t_1 - t_2 = \tau$, $t_2 = t$ in Eq. (3.13), we have, using the Wiener-Khintchine relationships

$$E[w(\bar{x}_1, t+\tau) \cdot w(\bar{x}_2, t)] = \frac{1}{2\pi} \sum_{n=1}^{\infty} \sin n\pi\bar{x}_1 \sin n\pi\bar{x}_2 \int_{-\infty}^{\infty} |H_w(n, \omega)|^2 S_f(\omega) e^{i\omega\tau} d\omega, \tag{3.15}$$

where $S_f(\omega)$ is the spectral density of the excitation process. For white-noise random excitation this remains constant over the entire frequency range. Denoting this value by S_0, the mean square displacement response of the system at a location $\bar{x}$ is obtained by putting $\bar{x}_1 = \bar{x}_2 = \bar{x}$ and $\tau = 0$ in Eq. (3.15),

$$E[w^2(\bar{x})] = \frac{S_0}{2\pi} \sum_{n=1}^{\infty} \sin^2 n\pi\bar{x} \int_{\infty}^{\infty} |H_w(n, \omega)|^2 d\omega. \tag{3.16}$$

If it is averaged over the space, then

$$E[w^2] = \frac{S_0}{4\pi} \sum_{n=1}^{\infty} \int_{-\infty}^{\infty} |H_w(n, \omega)|^2 d\omega. \tag{3.17}$$

The integral in Eq. (3.17) is evaluated by means of the method of residues and the general formula for evaluation of such integral is given in [14].

(ii) *Point load type*

Let the excitation process be stationary and of point load type acting at a single point $\bar{a}$ on the beam, then it can be expressed as

$$f(\bar{x}, t) = F(t)\, \delta(\bar{x} - \bar{a}). \tag{3.18}$$

Substituting Eq. (3.18) into Eq. (3.13) and simplifying with the aid of the Wiener-Khintchine relationships, we have mean square displacement at any point on the beam as

$$E[w^2(x)] = \frac{1}{\pi} \sum_{n=1}^{\infty} \sum_{m=1}^{\infty} \sin n\pi\bar{x} \sin m\pi\bar{x} \sin n\pi\bar{a} \sin m\pi\bar{a} \times \int_{-\infty}^{\infty} H_w(n, \omega) H_w(m, -\omega) S_f(\omega) d\omega. \tag{3.19}$$

On averaging over the space, the double summation will reduce to single summation because of the orthogonality of functions $\sin n\pi\bar{x}$ and $\sin m\pi\bar{x}$ and we have for white-noise excitation

$$E[w^2] = \frac{S_0}{2\pi} \sum_{n=1}^{\infty} \sin^2 n\pi\bar{a} \int_{-\infty}^{\infty} |H_w(n, \omega)|^2 d\omega. \tag{3.20}$$

3.3.2. Turbulent boundary layer random excitation

Measurements of wall pressure correlation by WILLMARTH [15], TACK *et. al* [16], BULL *et al.* [17], BAKEWELL [18] and CROCKER [19] indicate that

(a) the fluctuating pressure field is a random process which may be considered stationary in time and homogeneous in space, so that the pressure correlation is a function of spatial separations and time difference only, and

(b) the spatial correlation along each of the longitudinal and lateral directions can be represented by an exponentially damped cosine wave.

In view of (a) above, the correlation function of the turbulent boundary layer excitation can be expressed as

$$E[f(\bar{\xi}_1, \tau_1) \cdot f(\bar{\xi}_2, \tau_2)] = R_f(\bar{\zeta}, \tau_1 - \tau_2), \tag{3.21}$$

where $\bar{\zeta}$ = the spatial separation = $\bar{\xi}_1 - \bar{\xi}_2$. Substituting Eq. (3.21) in Eq. (3.13) and simplifying it with the aid of the Wiener-Khintchine relationships, we have

$$E[w(\bar{x}_1, t-\tau) \cdot w(\bar{x}_2, t)] = \frac{1}{\pi} \sum_{n=1}^{\infty} \sum_{m=1}^{\infty} \sin n\pi\bar{x}_1 \sin m\pi\bar{x}_2 \times \int_{-\infty}^{\infty} H_w(n, \omega) H_w(m, -\omega) e^{i\omega\tau} \int_0^1 \int_0^1 S_f(\bar{\zeta}, \omega) \sin n\pi\bar{\xi}_1 \sin m\pi\bar{\xi}_2 \, d\bar{\xi}_1 \, d\bar{\xi}_2 \, d\omega, \tag{3.22}$$

where the spectral density of pressure fluctuations is

$$S_f(\bar{\zeta}, \omega) = S_f(\omega) Q_f(\bar{\zeta}, \omega). \tag{3.23}$$

In view of (b) above

$$Q_f(\bar{\zeta}, \omega) = \exp(-\bar{\beta}_1 \bar{\zeta}) \cos(\bar{\gamma}\bar{\zeta}), \tag{3.24}$$

where [17, 19]

$$\bar{\beta}_1 = \frac{\omega L}{10 U_c}, \quad \bar{\gamma} = \frac{\omega L}{U_c}. \tag{3.25}$$

From Eq. (3.22) the mean square displacement at any point $\bar{x}$ is obtained as

$$E[w^2(\bar{x})] = \frac{1}{\pi} \sum_{n=1}^{\infty} \sum_{m=1}^{\infty} \sin n\pi\bar{x} \sin m\pi\bar{x} \int_{-\infty}^{\infty} S_f(\omega) H_w(n, \omega) H_w(m, -\omega) \times \int_0^1 \int_0^1 Q_f(\bar{\zeta}, \omega) \sin n\pi\bar{\xi}_1 \sin m\pi\bar{\xi}_2 \, d\bar{\xi}_1 \, d\bar{\xi}_2 \, d\omega \tag{3.26}$$

which, averaging over the space, reduces to

$$E[w^2] = \frac{1}{2\pi} \sum_{n=1}^{\infty} \int_{-\infty}^{\infty} S_f(\omega) |H_w(n, \omega)|^2 \int_0^1 \int_0^1 Q_f(\bar{\zeta}, \omega) \sin n\pi\bar{\xi}_1 \sin m\pi\bar{\xi}_2 \, d\bar{\xi}_1 \, d\bar{\xi}_2 \, d\omega. \tag{3.27}$$

Substituting for $Q_f(\bar{\zeta}, \omega)$ from Eq. (3.24) and introducing

$$\begin{cases} \bar{\xi}_1 + \bar{\xi}_2, = \bar{\eta}, \quad \bar{\xi}_1 - \bar{\xi}_2 = \bar{\zeta} \quad \text{and} \\ \sin n\pi\bar{\xi}_1 \sin n\pi\bar{\xi}_2 = \dfrac{1}{2}(\cos n\pi\bar{\zeta} - \cos n\pi\bar{\eta}) \end{cases} \tag{3.28}$$

in Eq. (3.27), and then applying a coordinate transformation similar to that suggested by CROCKER and WHITE [20], we get after simplification

$$E[w^2] = \frac{1}{4\pi} \sum_{n=1}^{\infty} \int_{-\infty}^{\infty} |H_w(n, \omega)|^2 S_f(\omega)(I_1 + I_2) d\omega, \tag{3.29}$$

where

$$I_1 = \frac{e^{-\bar{\beta}_1}\{-\bar{\beta}_1 \sin(n\pi+\bar{\gamma}) - (n\pi+\bar{\gamma})\cos(n\pi+\bar{\gamma})\} + n\pi(1+\bar{\beta}_1) + \bar{\gamma}}{n\pi\{(n\pi+\bar{\gamma})^2 + \bar{\beta}_1^2\}^2} + \frac{e^{-\bar{\beta}_1}[\{\bar{\beta}_1^2 - (n\pi+\bar{\gamma})^2\}\cos(n\pi+\bar{\gamma}) - 2\bar{\beta}_1(n\pi+\bar{\gamma})\sin(n\pi+\bar{\gamma})] - \bar{\beta}_1^2 + (n\pi+\bar{\gamma})^2}{[(n\pi+\bar{\gamma}^2) + \bar{\beta}_1^2]^2}, \tag{3.30}$$

I_2 is obtained from Eq. (3.30) simply by replacing $\bar{\gamma}$ by $-\bar{\gamma}$.

For $S_f(\omega)$ the Bull's model [20, 21] is used. This model or similar ones have been used by several authors [17, 19, 22] as the best empirical fits to the experimental data obtained by these authors from their investigations.

4. Influence of some geometrical and physical parameters on the displacement response

Figures 5 to 7 and 10 to 12 show the variation of the mean square displacement response with the coefficient of unsymmetry, core-thickness ratio and the elements of the model for white-noise random excitation.

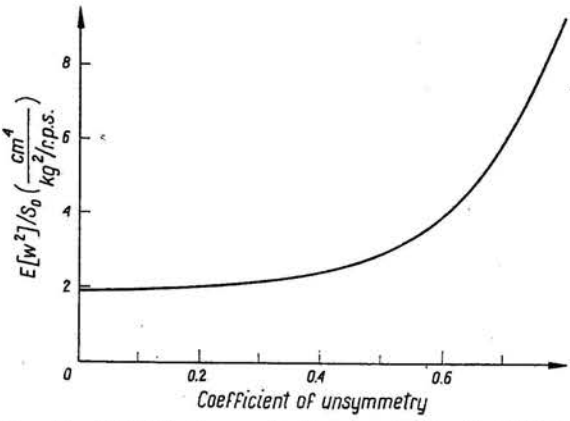

FIG. 5. Vibration of the ratio of M.S. displacement to force spectral density ($E[w^2]/S_0$) with the coefficient of unsymmetry.

Some of the parameters common to Figs. 5 to 7 and 10 to 12 are the following except the ones that have been varied in each case.

$$T_{1.3} = 1, \quad T_{2.3} = 1, \quad T_{3.L} = 0.0053, \quad \varrho_{1.3} = 1, \quad \varrho_{2.3} = 0.42857,$$
$$E_{1.3} = 1, \quad \varrho_3 = 0.28 \times 10^{-5} \text{kg sec}^2/\text{cm}^4, \quad E_3 = 7 \times 10^5 \text{ kg/cm}^2,$$
$$H_3 = 0.159 \text{ cm}, \quad b = 2.5 \text{ cm}, \quad \zeta_1/E_3 = 0.1314 \times 10^{-3}.$$

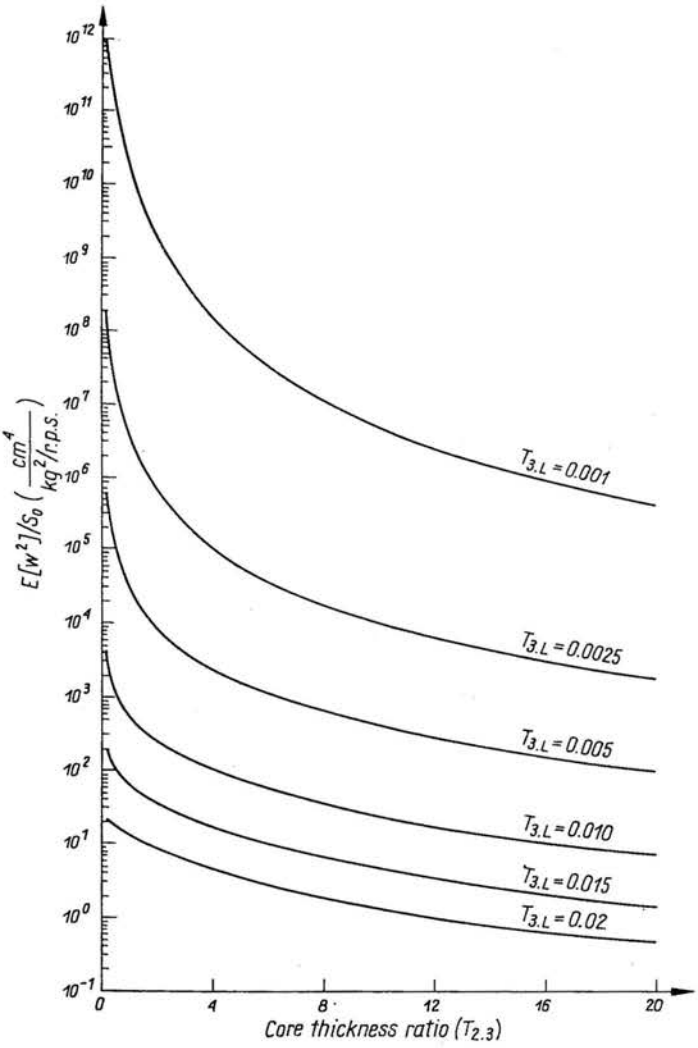

FIG. 6. Variation of the ratio of M.S. displacement to force spectral density ($E[w^2])S_0$) with $T_{2.3}$.

The coefficient of unsymmetry has been defined as the ratio $(H_3-H_1)/(H_3+H_1)$. The thicknesses $2H_1$ and $2H_3$ are varied while (H_1+H_3) is maintained constant. For a symmetrical configuration $H_1 = H_3$, this coefficient is zero. It is seen from Fig. 5 that the response ratio increases as the coefficient of unsymmetry increases and the least response is obtained for a symmetrical configuration. Figure 5 has been plotted for the above parameters except for $H_2 = 0.159$ cm and $(H_1+H_3) = 0.314$.

In Fig. 6 the response ratio is seen to decrease continuously with increasing values of $T_{2.3}$ initially at a faster rate at low values of $T_{2.3}$ and then at a slower rate for higher values of $T_{2.3}$. The initial rapid decrease of response is due to an increase of the overall loss factor of the beam with the increase of $T_{2.3}$. With a continued increase in $T_{2.3}$ the overall loss factor reaches a maximum and then decreases at a uniform rate [2]. This

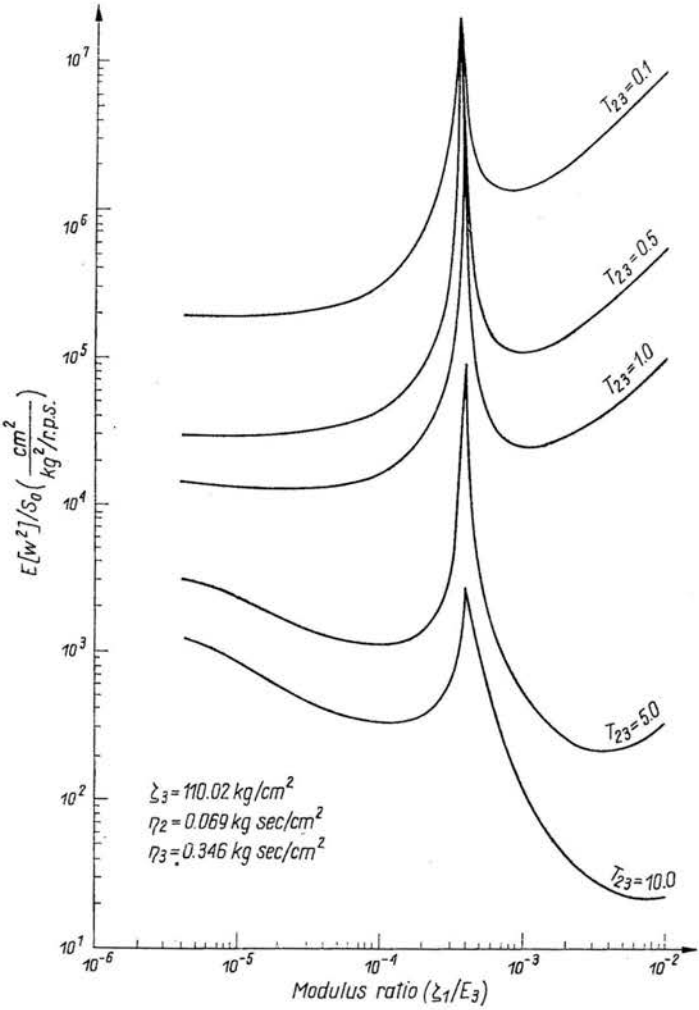

FIG. 7. Variation of the ratio of M.S. displacement to force spectral density ($E[w^2]/S_0$) with ζ_1/E_3.

decrease of the loss factor would tend to increase the response but this is offset by an increase in stiffness associated with the increase of $T_{2.3}$, thereby resulting in a slowly decreasing nature of the response for higher values of $T_{2.3}$.

Figure 7 shows the variation of the response ratio with increasing values of the modulus ratio ζ_1/E_3. It shows a typical behaviour of the response, which is unlike that for sinusoidal and impact excitations. This typical behaviour can be explained with the help of Figs. 8 and 9 which show the variation of the model loss factor and rigidity, respectively, with ζ_1 as the frequency of vibration is varied.

Corresponding to the data of Figs. 5 to 7, the first natural frequency of the sandwich beam with an elastic core and $G_2 = \zeta_1 = 210$ kg/cm^2, works out to be nearly 485 rad/sec. This is of interest since it is seen in Fig. 8 that the loss factor is low at about 485 rad/sec.

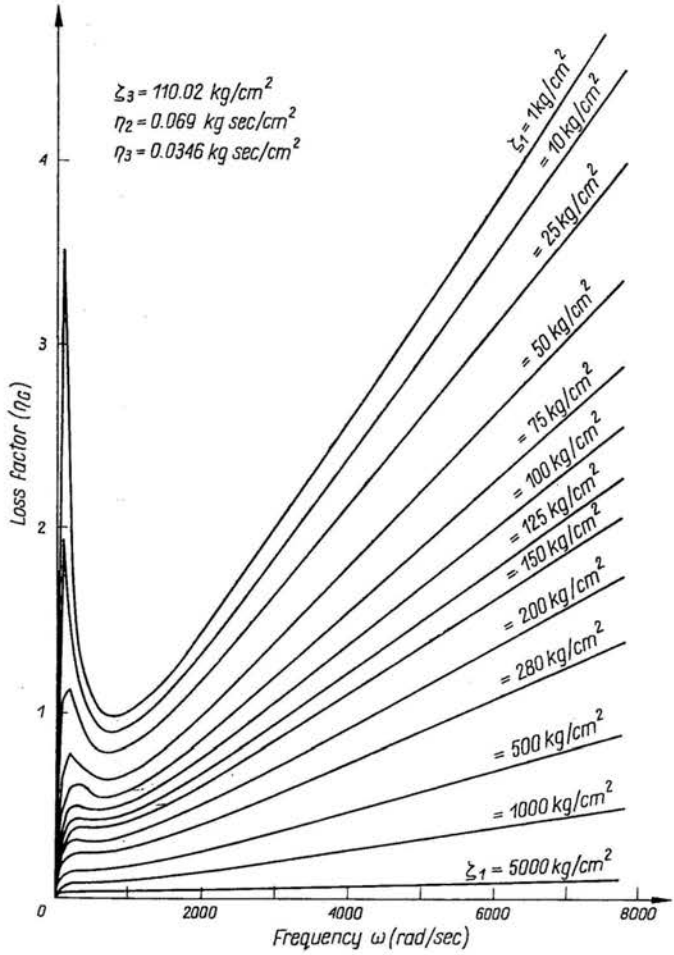

FIG. 8. Variation of η_G with ω and ϱ_1.

This minimal value of the loss factor results in the peak in Fig. 7 at $\zeta_1/E_3 = 3.0\times10^{-4}$, which corresponds to $\zeta_1 = 210$ kg/cm^2 because $E_3 = 7\times10^5$ kg/cm^2.

Figure 8 also shows that at all frequencies the loss factor is high at small values of ζ_1 and it decreases as ζ_1 increases. This fact results in a low value of the response at small values of ζ_1 and a subsequent increase of the response as ζ_1 increases till the response reaches the peak value as explained above.

The decrease of response from the peak value to a minimum is caused by the increase of rigidity (associated with increasing values of ζ_1 as shown in Fig. 9), which predominates over the effect of decrease of the loss factor associated with an increase of ζ_1. For the increase of response beyond the minimum, the effect of decrease of the loss factor predominates over the effect of increase in rigidity as the modulus ratio is further increased.

The variation of response with the other elements of the model, i.e. ζ_3, η_2 and η_3 is shown in Figs. 10 to 12. While the response is seen to decrease continuously with ζ_3 in

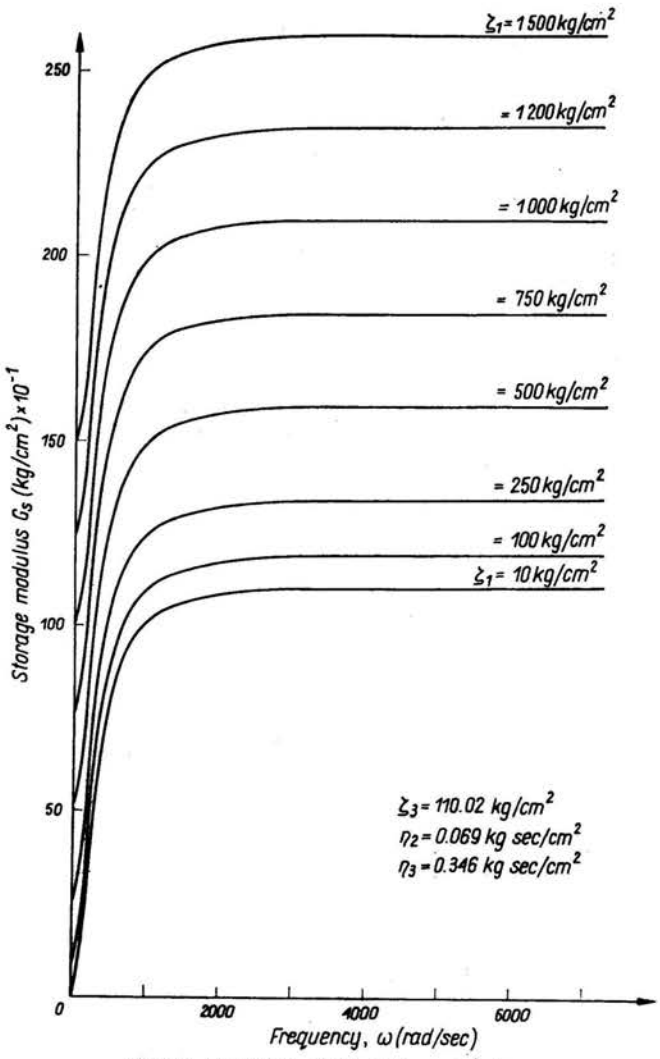

FIG. 9. Variation of G_s with ω and ζ_1.

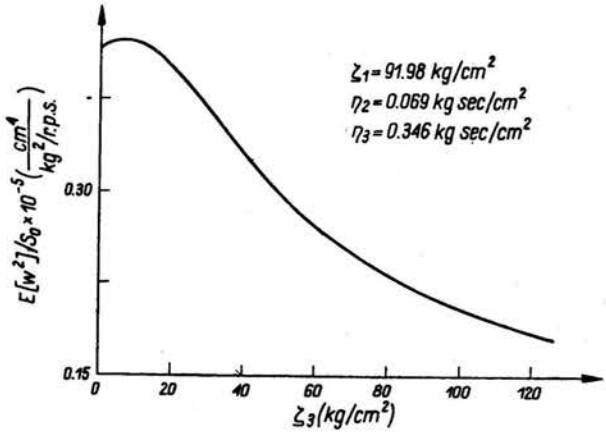

FIG. 10. Variation of the ratio of M. S. displacement to force spectral density ($E[w^2]/S_0$) with model element ζ_3.

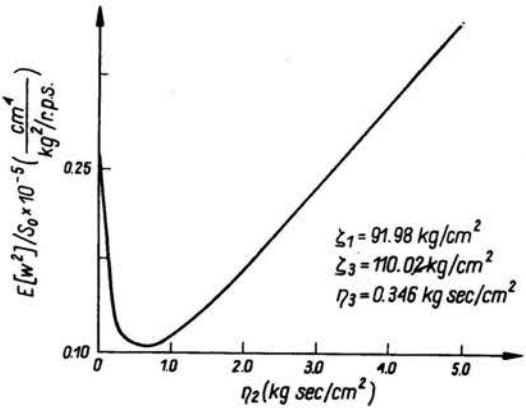

FIG. 11. Variation of the ratio of M.S. displacement to force spectral density ($E[w^2]/S_0$) with model element η_2.

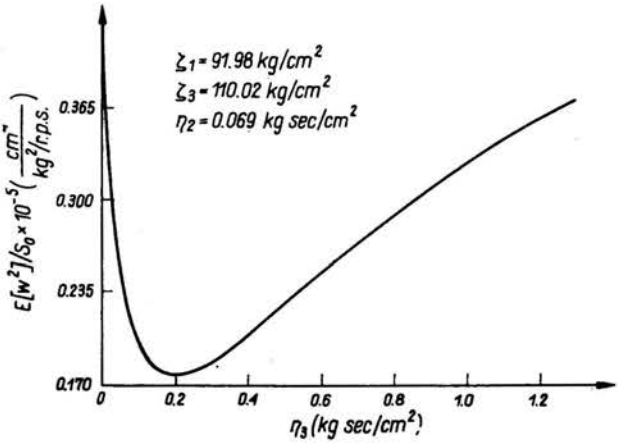

FIG. 12. Variation of the ratio of M.S. displacement to force spectral density ($E[w^2]/S_0$) with the model element η_3.

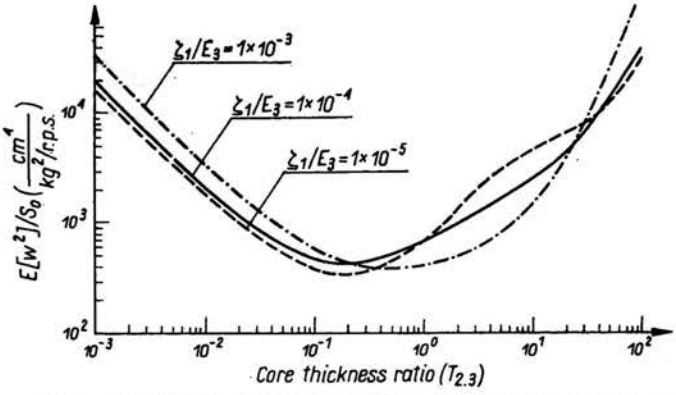

FIG. 13. Variation of the ratio of M. S. displacement to force spectral density ($E[w^2]/S_0$) with $T_{2,3}$ on constant size basis.

Fig. 10, it is seen to attain a minimum value with increasing values of η_2 and η_3 in Figs. 11 and 12. In these figures only one of the elements is varied at a time, while the other three are kept fixed.

In the case of turbulent boundary layer excitation, the results obtained are similar to those for white-noise excitation discussed above.

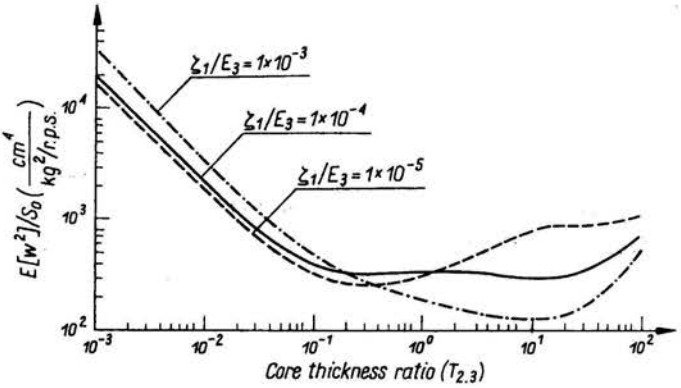

FIG. 14. Variation of the ratio of M. S. displacement to force spectral density $[E(w^2]/S_0)$ with $T_{2.3}$ on constant weight basis.

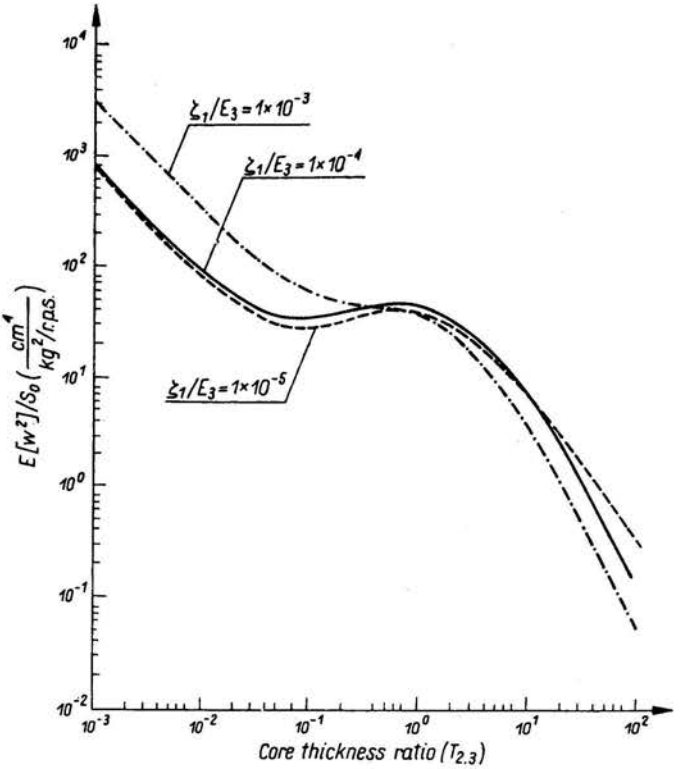

FIG. 15. Variation of the ratio of M.S. displacement to force spectral density $(E[w^2]/S_0)$ with $T_{2.3}$ on constant static stiffness basis.

5. Displacement response based on some design criteria

The evaluation of the displacement response based on the following criteria has been carried out.

a) Constant size criterion.

b) Constant weight criterion.

c) Constant static stiffness criterion.

For these criteria the performance of a three-layer sandwich beam (having face layers of equal thickness) is compared with that of a reference homogeneous beam whose material

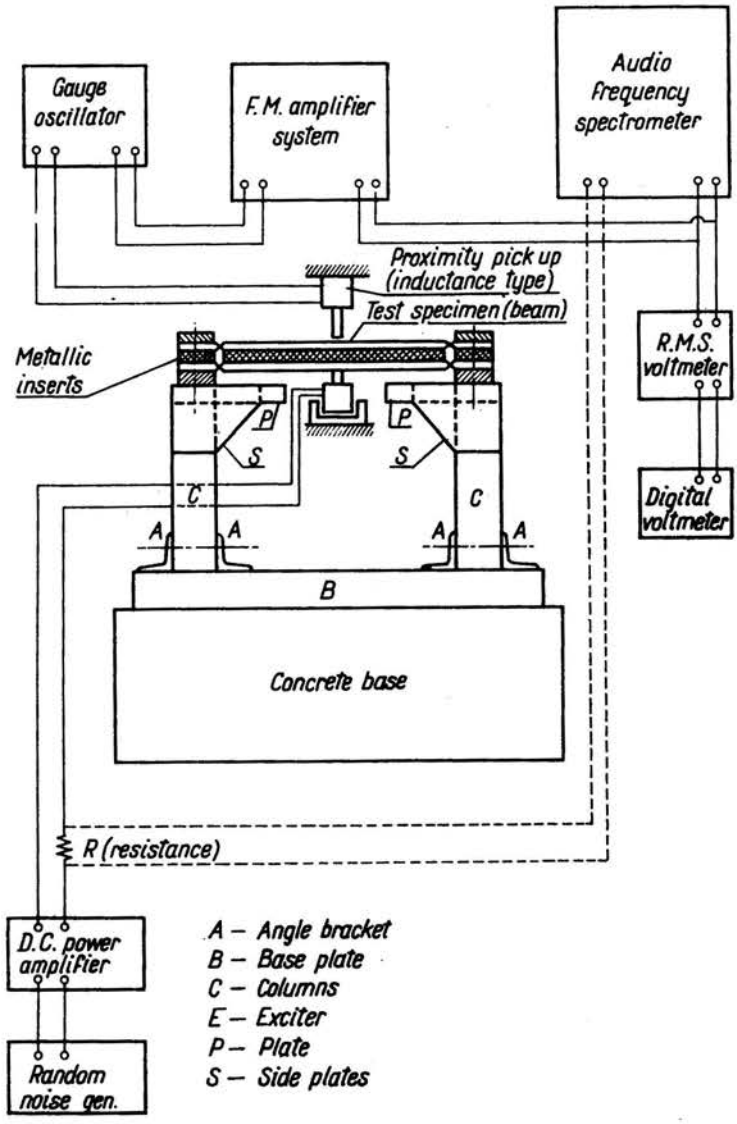

FIG. 16. Block diagram of testing equipment for white-noise random excitation.

is the same as that of the elastic face layers of the sandwich beam. For constant size, constant weight and constant static stiffness criteria, the thickness, weight and static stiffness, respectively, of a sandwich beam is taken equal to that of the reference beam.

The variation of these criteria with the core thickness ratio is given in [5]. The behaviour of response for each of these criteria under random excitation is shown in Figs. 13 to 15. It is seen from Figs. 13 and 14 that the response attains a minimum on constant size and the constant weight basis, whereas on the constant static stiffness basis the response decreases continuously for all values of $T_{2\cdot3}$ considered in Fig. 15.

6. Experimental work

Experiments were conducted on a few samples of the sandwich beams subjected to white-noise and turbulent boundary layer excitations. The block diagram of the testing

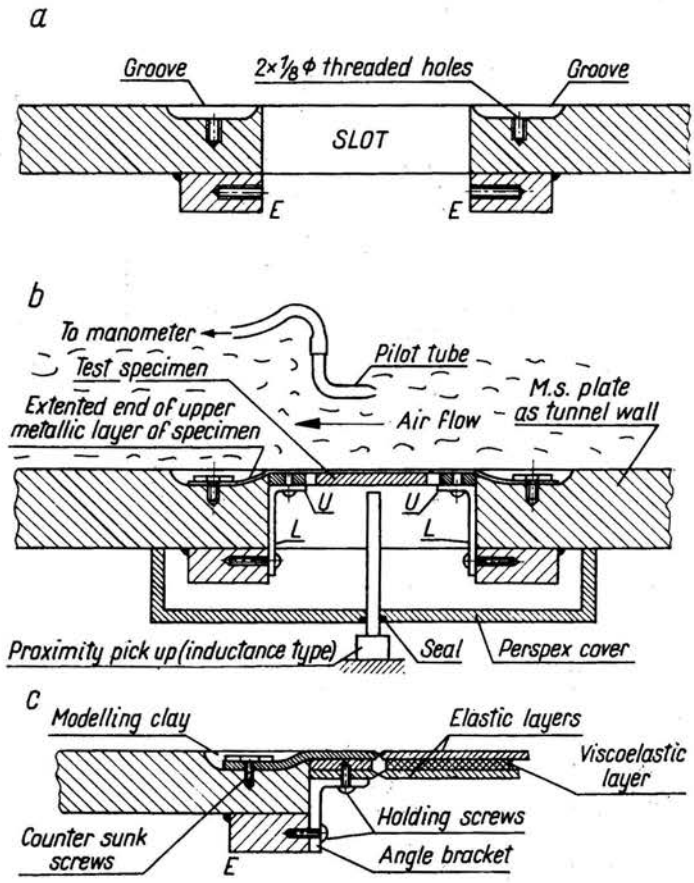

FIG. 17. Wind tunnel test section for turbulent boundary layer excitation. a) Details of slot and grooves in the mild steel wall-plate, b) Specimen in the wall-plate with box cover, pickup and pitot tube, c) Details of fixing of beam end.

equipment for white-noise random excitation is shown in Fig. 16. The ends of the test specimen are held in the clamps of the rigid stand which is placed over a concrete base. The specimen is excited at its mid-point by an exciter E held inside an annular magnet. It receives its power from a random noise generator through a d.c. power amplifier. The displacement response of the vibrating system sensed through a proximity inductance pick-up is fed through a F. M. amplifier system to a RMS voltmeter for measurement. The spectral density of excitation is measured with the help of an A. F. spectrometer as shown.

Experiments carried out on the sandwich beams to determine response to turbulent boundary layer excitation have been conducted on a 30 cm × 30 cm subsonic wind tunnel of the induced flow nonreturn type, driven by two exhaust fans down stream of the working section. The working section was suitably isolated from the exhaust section and the laboratory floor, so as to keep the vibrations of the test section to a minimum. To isolate further any vibrations of the tunnel wall itself due to air flow, a portion of the plywood wall of the tunnel was replaced by a 75 cm long mild steel plate in which a slot was cut to accommodate the test specimen as shown in Fig. 17. Details regarding the fixing of the beam ends and the positioning of the proximity pick-up are also shown therein. When the exhaust fans are switched on, the turbulent flow of air in the tunnel excites the specimen.

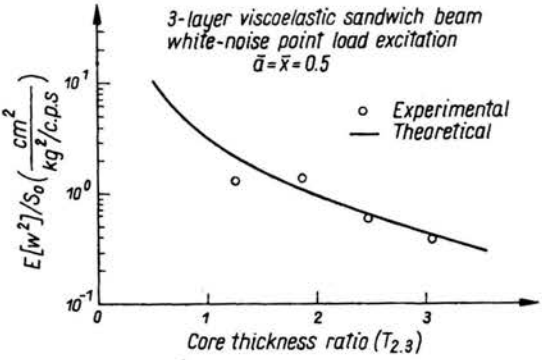

FIG. 18. Variation of the ratio of M.S. displacement to force spectral density ($E[w^2]/S_0$) with $T_{2.3}$.

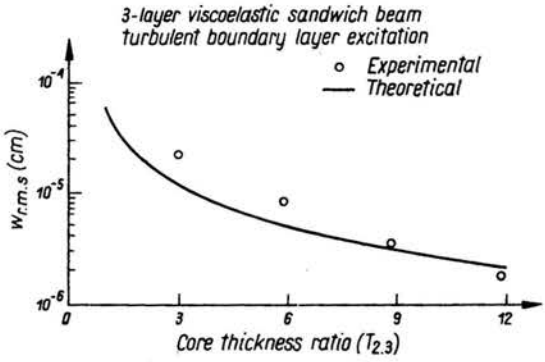

FIG. 19. Variation of R.M.S. displacement with $T_{2.3}$.

The displacement response is measured just in the same way as for the white-noise excitation case, whereas a manometer is used for measuring the pressure head so as to determine the velocity of air flow required for response calculations.

The details of the specimens, tested for both types of excitations and for which the results are being reported here, are given in Appendix A.

The experimental results and their corresponding theoretical values are shown in Figs. 18 and 19. A reasonable agreement between the experimental and theoretical results is seen.

Appedix A. Details of beam specimens tested

S. No.	L (cm)	b (cm)	Layer No. (i)	H_i (cm)	Material
A) White-noise random excitation					
1.	30	2.5	1	0.081	Al
			2	0.050	PVC
			3	0.081	Al
2.	30	2.5	1	0.081	Al
			2	0.100	PVC
			3	0.081	Al
3.	30	2.5	1	0.081	Al
			2	0.150	PVC
			3	0.081	Al
4.	30	2.5	1	0.081	Al
			2	0.200	PVC
			3	0.081	Al
B) Turbulent boundary layer excitation					
1.	13	2.5	1	0.017	Al
			2	0.050	PVC
			3	0.017	Al
2.	13	2.5	1	0.017	Al
			2	0.100	PVC
			3	0.017	Al
3.	13	2.5	1	0.017	Al
			2	0.150	PVC
			3	0.017	Al
4.	13	2.5	1	0.017	Al
			2	0.200	PVC
			3	0.017	Al

7. Conclusions

The mean square displacement response is minimum for a symmetrical beam and it increases as the unsymmetry increases. As the core thickness increases, the response decreases rapidly at lower values and gradually for larger values of the core thickness.

The variation of the response with the elements of the model shows that it is possible to find such values for these elements individually, so as to give rise to a minimum or a low value of the response, while the other three elements are kept fixed. This fact will be helpful in designing the viscoelastic sandwich beam for obtaining a predetermined value of response by specifying the values of elements of the model for the viscoelastic core material.

References

1. P. GROOTENHUIS, *Damping mechanisms in structures and some applications of the latest techniques*, Proc. Symp. on Applications of Experimental and Theoretical Structural Dynamics, Southampton University, 17.1–17.17, 26th April 1972.
2. D. ROSS, E. E. UNGAR and E. M. KERWIN Jr., *Damping of plate flexural vibrations by means of viscoelastic laminae*, ASME publication, Structural Damping, Section 3, New York 1959.
3. H. OBERST, *Über die Dämpfung der Biegeschwingungen dünner Bleche durch fest haftende Beläge, Pt. I.* Acustica, **2**, 4, 1952; and Pt. II. Acustica, **4**, 1, 1954.
4. R. A. DI TARANTO, *Theory of vibratory bending for elastic and viscoelastic layered finite length beams*, J. Appl. Mech., **32**, 4, 881–886, 1965.
5. N. T. ASNANI and B. C. NAKRA, *Vibration damping of multilayered beams with constrained viscoelastic layers*, J. Engg. for Industry, paper 73-DE-C, ASME publication, 1973.
6. J. A. AGBASIERE and P. GROOTENHUIS, *Flexural vibrations of symmetrical multilayer beams with viscoelastic damping*, J. Mech. Eng., Sc., **10**, 3, 269–281, 1968.
7. I. W. JONES, *Non-periodic vibrations of layered viscoelastic plates*, Ph. D. Dissertation, Poly, Inst. of Brooklyn 1967.
8. A. D. KAPUR, *Vibration response of multilayer beams subjected to shock excitation*, Ph. D. thesis, Indian Institute of Technology, Delhi, 1974.
9. D. J. MEAD, *The effect of a damping compound on jet-efflux excited vibrations, Pt. I. The structural damping due to the compound*, J. Aircraft Eng., **32**, 373, 64–72, 1960. *Pt. II. Reduction of vibration and stress level due to the compound*, **32**, 374, J. Aircraft Eng., 106–113, 1960.
10. H. SAUNDERS, *Response of a multi-layer plate to random excitation*, Shock and Vib. Bulletin, **42**, Pt. 5, 27–35, 1972.
11. O. N. KAUL, K. N. GUPTA and B. C. NAKRA, *Response of a viscoelastic sandwich beam to white-noise random excitation*, Presented at XVIII Congress ISTAM, Madras, 1973.
12. O. N. KAUL, *Vibration response of multilayer structures to random excitation*, Ph. D. Thesis, Indian Institute of Technology, Delhi 1976.
13. S. H. CRANDALL and A. YILDIZ, *Random vibration of beams*, J. Appl. Mech., **29**, 2, 267–275, 1962.
14. I. S. GRADSHTEYN and J. M. RYZHIK, *Tables of integrals, series and products*, Translated from the Russian, Academic Press, 218–219, 1965.
15. W. W. WILMIRTH, *Space-time correlation and spectra of wall pressure in a turbulent boundary layer*, NASA Memo 3-17-59W, 1959.
16. D. H. TACK, M. W. SMITH and R. F. LAMBERT, *Wall pressure correlation in turbulent air flow*, J. Acoust. Soc. Amer., **33**, 4, 410–418, 1961.
17. M. K. BULL, J. F. WILBY and D. R. BLACKMAN, *Wall pressure fluctuations in boundary layer flows and response of simple structures to random pressure fields*, Univ. of Southampton, Report A.A.S.U., 243, 1963.

18. H. P. BAKEWELL, *Longitudinal space-time correlation function in turbulent air flow*, J. Acoust. Soc. Amer., **35**, 6, 936–937, 1963.
19. M. J. CROCKER, *The response of a supersonic transport fuselage to boundary layer and to reverberrant noise*, J. Sound and Vib., **9**, 1, 6–20, 1969.
20. M. J. CROCKER and R. W. WHITE, *Response of uniform beams to homogeneous random pressure fields*, J. Acoust. Soc. Amer., **45**, 5, 1097–1103, 1969.
21. M. K. BULL, *Wall pressure fluctuations associated with subsonic turbulent boundary layer flow*, J. Fluid Mech., **28**, Pt. 4, 719–754, 1967.
22. L. MAESTRELLO, *Use of turbulent model to calculate the vibration and radiating responses of a panel—with practical suggestions for reducing sound level*, J. Sound and Vib., **5**, 3, 407–448, 1967.

INDIAN INSTITUTE OF TECHNOLOGY, NEW DELHI, INDIA.

Received October 3, 1978.